Journal Pre-proof

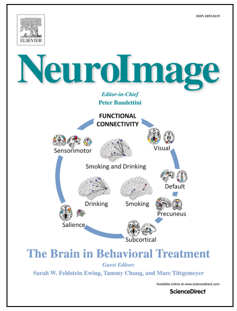

Neural underpinnings of value-guided choice during auction tasks: An eye-fixation related potentials study

John Tyson-Carr, Vicente Soto, Katerina Kokmotou, Hannah Roberts, Nicholas Fallon, Adam Byrne, Timo Giesbrecht, Andrej Stancak

PII: S1053-8119(19)30804-3

DOI: https://doi.org/10.1016/j.neuroimage.2019.116213

Reference: YNIMG 116213

To appear in: *NeuroImage*

Received Date: 21 June 2019

Revised Date: 14 September 2019

Accepted Date: 18 September 2019

Please cite this article as: Tyson-Carr, J., Soto, V., Kokmotou, K., Roberts, H., Fallon, N., Byrne, A., Giesbrecht, T., Stancak, A., Neural underpinnings of value-guided choice during auction tasks: An eye-fixation related potentials study, *NeuroImage* (2019), doi: https://doi.org/10.1016/j.neuroimage.2019.116213.

Neural underpinnings of value-guided choice during auction tasks: an eye-fixation related potentials study

John Tyson-Carr[1], Vicente Soto[1,2], Katerina Kokmotou[1], Hannah Roberts[1], Nicholas Fallon[1], Adam Byrne[1], Timo Giesbrecht[3], Andrej Stancak[1]

[1] Department of Psychological Sciences, University of Liverpool, Liverpool, UK.

[2] Center for Social and Cognitive Neuroscience (CSCN), School of Psychology, Universidad Adolfo Ibañez, Santiago, Chile.

[3] Unilever Research and Development, Port Sunlight, UK.

Corresponding author:

John Tyson-Carr

Department of Psychological Sciences

University of Liverpool

Liverpool, L69 7ZA

United Kingdom

Email: hljtyson@liverpool.ac.uk

Phone: +44 151 794 6956

Keywords: Becker-DeGroot-Marschack auction; independent component analysis; value-based decision making; willingness to pay; evoked potentials

Abstract

Values are attributed to goods during free viewing of objects which entails multi- and trans-saccadic cognitive processes. Using electroencephalographic eye-fixation related potentials, the present study investigated how neural signals related to value-guided choice evolved over time when viewing household and office products during an auction task.

Participants completed a Becker-DeGroot-Marschak auction task whereby half of the stimuli were presented in either a free or forced bid protocol to obtain willingness-to-pay. Stimuli were assigned to three value categories of low, medium and high value based on subjective willingness-to-pay. Eye fixations were organised into five 800 ms time-bins spanning the objects total viewing time. Independent component analysis was applied to eye-fixation related potentials.

One independent component (IC) was found to represent fixations for high value products with increased activation over the left parietal region of the scalp. An IC with a spatial maximum over a fronto-central region of the scalp coded the intermediate values. Finally, one IC displaying activity that extends over the right frontal scalp region responded to intermediate- and low-value items. Each of these components responded early on during viewing an object and remained active over the entire viewing period, both during free and forced bid trials.

Results suggest that the subjective value of goods are encoded using sets of brain activation patterns which are tuned to respond uniquely to either low, medium, or high values. Data indicates that the right frontal region of the brain responds to low and the left frontal region to high values. Values of goods are determined at an early point in the decision making process and carried for the duration of the decision period via trans-saccadic processes.

1. Introduction

Selecting appropriate courses of action entails a value assignment process wherein the most subjectively beneficial action is selected (Rangel et al., 2008). Being a function of momentary needs, value itself is unique to the individual and is typically revealed via behavioural measures (Schultz, 2017), such as auction tasks. The Becker-DeGroot-Marschak (BDM) auction (Becker et al., 1964) is from a class of incentive compatible methods that reveal participant willingness-to-pay (WTP) for goods and prospects (Wilkinson and Klaes, 2012). BDM auctions have been often utilised in value-based decision making research (Chib et al., 2009; Grueschow et al., 2015; Hare et al., 2008; Harris et al., 2011; Peters and Buchel, 2010; Plassmann et al., 2007, 2010; Weber et al., 2007), though a variety of methods for prompting unique valuations are employed (see Peters and Büchel, 2010).

Neuroeconomic research has posited the explicit representation of value signals in the brain (Glimcher and Fehr, 2014), with the ventromedial prefrontal cortex, orbitofrontal cortex (OFC) and ventral striatum playing prominent roles (Bartra et al., 2013; Chib et al., 2009; Clithero and Rangel, 2014; Lebreton et al., 2009; Levy and Glimcher, 2012). Valuation appears to be largely an automatic process which resolves values even if people focus on value-irrelevant aspects of objects such as perceptual features (Grueschow et al., 2015; Polania et al., 2014; Tyson-Carr et al., 2018), or when subjects are not required to valuate items (Plassmann et al., 2007, 2010). Although BOLD-fMRI methods excel in terms of spatial resolution to isolate brain regions responsible for economic valuation, these methods are limited by the temporal resolution which allows tracking brain activation on a scale of seconds (Shmuel and Maier, 2015).

Capitalising on the high temporal resolution of electrophysiological methods, electroencephalography (EEG) has aimed to show the temporal dynamics of value-based decisions, though research is sparse. Event-related potential (ERP) signals have been shown to represent value in binary decision tasks, even as early as 150 ms post-stimulus (Harris et al., 2011; Larsen and O'Doherty, 2014; Tzovara et al., 2015). It has also been demonstrated that activation may progress from occipito-temporal regions to frontal regions of the scalp over time following stimulus presentation (Harris et al., 2011; Larsen and O'Doherty, 2014). Our recent study (Tyson-Carr et al., 2018) revealed that a visual evoked potential component within the latency of N2 and originating in the right anterior insula was preferentially activated with items having low subjective values. Moreover, Roberts et al. (2018) reported that the parietal P200 eye movement-related potential may index attention to low value products in a realistic setting. Similarly, magnetoencephalographic methods have also been used to classify the neural mechanism of value-guided choices (Hunt et al., 2012). In addition to the initial value attribution stage, outcome specific modulation of ERPs have also been observed in the P300, which may encode valence (San Martin, 2012; Yeung and Sanfey, 2004), and also the event- and feedback-related negativity which may be linked to reward-prediction errors (Gehring et al., 2012; Nieuwenhuis et al., 2004; Yu and Huang, 2013).

While previous fMRI and ERP studies shed light on spatial and temporal aspects of valuation during economic decision making, the detailed dynamics of the valuation process that evolve while an object is being viewed is poorly understood. When people evaluate objects to make economic decisions, their valuation evolves during free viewing of a visual scene. In free viewing, one or more objects in the visual field are explored in a series of saccades and fixations concatenated by trans-saccadic integration mechanisms (Melcher and Colby, 2008). Objects of greater value or those having a pleasant emotional connotation tend to be viewed for a longer time than objects of low value or aversive stimuli (Krajbich et al., 2010; van der Laan et al., 2015). If values are attributed to objects automatically, the assignment of an object to a high or low subjective value category would be captured by the brain early on during the viewing process and, once established, the value category would persist throughout the viewing period. In contrast, if values are attached to objects only after a careful exploration, purportedly involving volitional effort, objects would be assigned a provisional value, e.g., suggested initially by the automatic valuation process, but this value would be updated over a series of successive eye fixations. In such case, information about brain valuation while people are viewing objects before they decide to purchase would likely be encoded in the cortical responses to eye fixations, occurring just before a purchasing decision is made.

Eye-fixation related potentials (EFRPs) allow for the unveiling of neural processes at the point of fixation (Baccino and Manunta, 2005), and are often utilised during the free reading of words or viewing of scenes (Dimigen et al., 2011; Fischer et al., 2013; Hutzler et al., 2007; Nikolaev et al., 2016; Simola et al., 2015). BOLD-fMRI lacks the temporal resolution necessary to investigate the brain processes occurring on a scale of hundreds of milliseconds, and averaged ERPs only pick up information about the cortical activations occurring in the initial stage of valuation locked to the onset of visual stimulus. To overcome both of these shortcomings, EFRPs can provide a window into the cortical activations occurring over the entire period of free viewing accompanying the valuation.

Firstly, following up on our previous study (Tyson-Carr et al., 2018), we predicted that one activation component localised across the right frontal region of the scalp would encode low-value items. Since the range of products was expanded in the high-value interval in the present study (£0 - £8) compared to our previous study (£0 - £4; Tyson-Carr et al., 2018), it was also hypothesised that other components would encode high- or medium-value items independently of the low-value sensitive component. Based on previous studies reporting the latency of value-based decision processes within the range of the N2 visual-evoked potential component (Harris et al., 2011; Kiss et al., 2009; Larsen and O'Doherty, 2014; Telpaz et al., 2015), we hypothesised that value encoding would occur in the latency of the N2 EEG component. Secondly, it was hypothesised that due to automaticity of valuation demonstrated in a number of previous studies (Grueschow et al., 2015; Lebreton et al., 2009; Plassmann et al., 2007, 2010; Polania et al., 2014), components would categorise the value of objects during initial eye fixations and maintain activations in subsequent eye fixations throughout the viewing period; the automaticity of value-based decision making would manifest in similarity of activation profiles over the viewing period for forced and free bids.

2. Methods

2.1. Participants

Twenty-four healthy participants (16 females) with a mean age of 25 ± 5.06 (mean ± SD) years took part in the study. The experimental procedures were approved by the Research Ethics Committee of the University of Liverpool. All participants gave written informed consent in accordance with the declaration of Helsinki. Participants were reimbursed for their time and travel expenses. Due to technical issues with eye-tracking data, 6 participants were excluded, thus data from 18 participants were submitted for analysis.

2.2. Procedure

All experimental procedures were carried out in a dimly lit, sound attenuated room. Participants sat in front of a 19-inch LCD monitor. The study was carried out in a single experimental session involving the completion of an auction task. The stimuli included 180 everyday household items varying in value from £0.35 to £8.00 with a mean value of £4.30 ± 2.41 obtained from a shopping catalogue. Stimuli were presented in random order. Presentation of stimuli was controlled using Cogent 2000 (UCL, London, UK) in Matlab 7.8 (Mathworks, Inc., USA).

2.3. EEG recordings

EEG was recorded continuously using the 128-channel Geodesics EGI system (Electrical Geodesics, Inc., Eugene, Oregon, USA) with the sponge-based HydroCel Sensor Net. The sensor net was aligned with respect to three anatomical landmarks (two pre-auricular points and the nasion). Electrode-to-skin impedances were kept below 50 kΩ across all electrodes as recommended for the system (Picton et al. 2000; Ferree et al. 2001; Luu et al. 2003). The sampling rate was 1000 Hz and electrode Cz was used as the initial reference. The recording bandpass-filter was 0.1-200 Hz.

2.4. Eye-tracking recordings

Gaze positions were monitored using the Pupil head-mountable binocular eye-tracker (Kassner et al., 2014). Eye-cameras ran at a sampling rate of 120 Hz and the world camera at 60 Hz. Gaze tracking was calibrated using a 9-point manual marker calibration protocol in which calibration markers were presented sequentially on the stimulus presentation monitor. Following calibration, gaze position accuracy was tested using a program that presented markers randomly on the screen for the participant to track. If gaze position was not easily discernible, calibration was repeated, otherwise the experiment was continued. Pupil Capture software v 0.8.1 was used for data collection. Pupil Player software v 0.8.6 running in Xubuntu was used for data visualisation and raw data exporting.

During the auction task, a series of digital fiducial surface markers were placed in each corner of the screen in order to define the surface of the monitor display. These markers were displayed continuously throughout the trials. Offline surface detection was carried out post data-collection but prior to fixation detection to allow fixations to be localised relative to the surface.

2.5. Auction task

The protocol (see Figure 1) for the auction task was adapted from previous studies (Plassmann et al., 2007, 2010) and employed the BDM mechanism (Becker et al. 1964; Wilkinson and Klaes 2012). Each stimulus was presented once in either a free bid or forced bid protocol, resulting in a total of 180 auctions.

Each auction consisted of a fixation cross followed by an evaluation stage, a bidding phase and then feedback. During the evaluation stage, participants appraised the stimulus. Afterwards, they were required to bid between £0 and £8 using a mouse to select the appropriate option on the screen. Bidding options were in increments of £0.50 between £0 and £2 and in increments of £1 between £2 and £8. This allowed more resolution at lower ends of the value scale, thus giving a total of 11 options. Participants clicked an orange square once satisfied with their bid. The screen had a horizontal size of 38.8º and vertical size of 34.7º when participants were viewing at a distance of 65 cm, stimuli had a horizontal and vertical size of 19.5º and the bidding scale had a horizontal size of 34.5º and vertical size of 2.3º.

After bid selection, feedback was provided as to whether the item was purchased or not. The outcome of an auction was dependent on the bid and a randomly generated number, in which the item was purchased when $b \geq r$, where *b* represents the bid and *r* represents the randomly generated number for that auction. Following the experiment, one of the auctions that resulted in a purchase were selected at random and the outcome was implemented. Here, the participant's endowment of £8 was reduced by an amount equal to *r* for the implemented auction. The item purchased could be picked up within a few days of completion of the experiment.

Half of the stimuli were presented in the free bid condition whereas the other half were presented in the forced bid condition. In the free bid condition, participants were presented with a question mark above the bid amounts, indicating that they are free to bid whatever they like for the item. In the forced bid condition, participants were presented with a monetary amount above the bid amounts to indicate what they are required to bid for the item. Here, the participant cannot select any other option and cannot continue until they have selected that option. The only difference between these two conditions is the need for a computation of value.

After the main auction task, another auction task was conducted without recording EEG in order to obtain subjective WTP values for the items presented in the forced bid protocol. This is to allow categorisation of stimulus value that is not represented by a trivial forced bid procedure in which they have no influence over the reported value.

2.6. Split of WTP values

The stimulus set was divided into three groups of high, medium and low subjective value products for both the free bid and forced bid stimuli. To avoid overlapping values between these conditions, stimuli were removed randomly so that there were six groups of equal size (free bid and low / medium / high value; forced bid and low / medium / high value), with each value category containing unique WTP values that did not overlap with any other value category. An average of 118 ± 17.3 trials were submitted for analysis for each subject, giving 19.7 ± 2.88 trials per condition.

The splitting of WTP into three categories was decided based on our previous study (Tyson-Carr et al., 2018) which included a stimulus set that was comprised of a relatively small range of subjective values (£0 to £4), split into two value categories of low and high value. The expansion of the stimulus value range to between £0 and £8 afforded us the ability to include a third value category comprised of products with intermediate WTP, increasing the ability to capture brain components for distinct increments of value. An increased number of value categories was not possible due to limited numbers of epochs.

2.7. EEG pre-processing

EEG data were pre-processed using BESA v. 6.1 program (MEGIS GmbH, Munich, Germany). EEG data were spatially transformed to reference-free data using common average reference method (Lehmann, 1984). Oculographic artefacts and electrocardiographic artefacts were removed using principle component analysis based on averaged eye-blinks and artefact topographies (Berg and Scherg, 1994). Data were also visually inspected for the presence of atypical electrode artefacts occurring due to muscle movement. Data were filtered from 0.5-45 Hz and exported to EEGLab (Delorme and Makeig, 2004) for further processing.

2.8. Detection of eye fixations

Fixations were detected based on the given parameters of 150 ms minimum duration and a 1° dispersion threshold (Blignaut, 2009). Each subject made on average 3965 ± 792 (mean ± SD) fixations on the screen across the experiment. Next, only fixations occurring during image presentation were accepted, resulting in 1725 ± 299 fixations. Following the splitting of stimuli into three value categories and the required exclusion of overlapping stimuli, fixations occurring during trials of excluded stimuli were also removed, resulting in 1154 ± 222 fixations. Given the two trial types accompanying the three value conditions, this resulted in a mean of 192 ± 5.4 fixations for each of the six conditions. Fixations overlapping with artefacts within the EEG data were also removed, resulting in 171 ± 4.6 fixations per condition. In addition to the six conditions, fixations were also organised into five time bins. These time bins were classified based on five 800 ms intervals encompassing the 4000 ms of image presentation. This allowed the organisation of fixations into five discrete and equally spaced categories between image onset and offset. These categories will be referred to as TB1, TB2, TB3, TB4 and TB5 hereafter. Since the data was also split into five time bins, this further reduced the number of fixations per condition to 34 ± 2.44 fixations and 8.76 ± 1.5 fixations per trial for every subject submitted for analysis.

2.9. Eye-fixation related potential analysis

Since EEG and eye-tracking was recorded with separate systems, the data had to be synchronised. A TTL pulse inputted into the EEG data stream indicating image onset and the corresponding appearance of the image in the word-view camera of the eye-tracking allowed for synchronisation.

After synchronising eye-tracking and EEG data, EFRPs in response to fixation onset were computed separately for each level of value condition (low, medium, high), trial type (free, forced) and time bin (TB1, TB2, TB3, TB4, TB5) by averaging respective epochs in the intervals ranging from 200 ms before fixation onset to 400 ms following fixation onset. Epochs were baseline corrected using an individual baseline in the time window of -200 to -100 ms relative to fixation onset (Luck, 2005). This baseline was selected to mitigate effects of the saccadic spike potential (SP). Given the modulation of the SP by a variety of eye-movement characteristics, baselines encompassing the SP may induce differences between conditions due to condition specific eye-movements (Nikolaev et al., 2016).

2.10. Eye-movement characteristics

Since eye-movement characteristics can modulate the pre-saccadic activity, the SP and the lambda brain potentials, eye-movement characteristics were analysed (Boylan and Doig, 1989; Keren et al., 2010; Nikolaev et al., 2016; Riemslag et al., 1988; Thickbroom and Mastaglia, 1986). Saccade amplitude was defined as the gaze distance between saccade initiation and fixation onset, expressed in degrees of visual angle, for each fixation. Saccade direction represented the angle between these two points for each fixation.

2.11. Component clustering

EFRPs were input into the EEGLab (Delorme and Makeig, 2004) STUDY structure to allow for the clustering of similar independent components (ICs) across subjects. Independent component analysis (ICA) was first carried out on the concatenated epochs for each subject to identify a set of ICs. Next, ERP and scalp map component measures were computed and used to build a pre-clustering array for clustering components into 18 clusters. Clustering into 18 clusters was chosen to reflect the number of participants submitted for analysis to allow independent components to be distributed amongst an appropriate number of clusters for a suitable separation of brain components. To restrict analysis to the most significant clusters, 95% confidence intervals were computed on the time course of each cluster. If the confidence intervals did not exceed zero, i.e. the interval overlaps with zero, the cluster was excluded.

2.12. Unfold toolbox

Free-viewing in EEG paradigms allow us to examine neural processes over an extended period of time. However, the introduction of free-viewing is accompanied by overlapping neural responses from subsequent fixation events. Thus, any value- or condition-related changes in EFRPs may be confounded by associated eye-movements. To control for the impacts of eye movements on EFRPs, the Unfold toolbox (Ehinger and Dimigen, 2018) was employed. This toolbox uses linear deconvolution to isolate the neural response from events with varying temporal overlap.

To ensure that the changes in IC clusters were not a result of saccadic eye-movements occurring within the latency of each epoch, each IC cluster was back projected onto the continuous EEG data and analysed using the Unfold toolbox to test for the influence of overlapping potentials on the data (see Supplementary materials). Firstly, a linear model was defined for the linear deconvolution procedure to estimate potentials across all fixations. Since we were not interested in the potentials for each condition, but rather the grand average deconvolution, the potentials for each condition were not modelled here. Next, a regression analysis was applied to the continuous EEG data using the following formula:

$$EEG = X_{dc}b + e \quad \text{(Eq. 1)}$$

where X_{dc} encodes covariates for all time samples in the continuous EEG data, b contains the regression (beta) coefficients and e the residuals. Next, the regression formula was solved for the beta (b) coefficients, wherein these betas represented non-overlapping potentials. Since our model did not include terms for any condition, the intercept represented the de-convolved brain potentials for each IC cluster.

3. Results

3.1. Behavioural data

Mean WTP values were computed for each condition separately. In the free bid trials, a mean value of £0.71 ± £0.64 was observed for low value items, £2.23 ± £1.14 for medium value items and £5.02 ± £1.50 for high value items. In the forced bid trials, a mean WTP value of £0.76 ± £0.85 was observed for low value items, £1.99 ± £1.44 for medium value items and £4.31 ± £1.80 for high value items.

All value categories were significantly different from each other (P < .001). There was also a significant difference between free and forced bid trials, $F(1,17) = 8.84$, $P = .009$, $\eta_p^2 = .342$, as well as an interaction between value and trial type, $F(2,34) = 18.9$, $P < .001$, $\eta_p^2 = .526$. Pairwise comparisons reveal a significant difference between medium value items for free and forced bids, $t(17) = 2.31$, $P = .037$, $d = 0.19$, and also between high value items, $t(17) = 4.15$, $P < .001$, $d = 0.43$. Given that this could potentially confound results when interpreting any main effect or interaction including trial type, these analyses will have the addition of a covariate analysis with WTP values.

3.2. Fixation location data

The mean saccade amplitude for each condition was calculated and input into a 3 (values) * 2 (forced vs. free) * 5 (time bins) ANOVA for repeated measures. There were no significant main effects or interactions between conditions for saccade amplitude.

The circular nature of saccade direction required statistical testing appropriate for circular statistics. The mean circular saccade direction for each subject and condition was calculated using the CircStat toolbox (Berens, 2009) before being analysed using the bpnreg package (Cremers and Klugkist, 2018) implemented in R (R Core Team, 2018). A mixed effects model was fitted to assess the interaction between value category, trial type and time bin regarding the circular outcome of saccade direction. This analysis produced the 95% highest posterior density (HPD) intervals, an interval allowing probability statements about the parameters, displayed in Figure 2. Inspection of the intervals reveal overlapping intervals between all value categories, within all time bins, for both free and forced bids, with the exception of time bin 2 for free bids wherein low value products elicited different saccade directions. We therefore conclude that saccade direction was only intermittently different between conditions, given the overlapping distributions of circular mean directions.

To aid in the interpretation of EFRPs, fixation data across the screen was converted into a 40*40 bivariate histogram to visualise the locations of fixations for each condition. During the evaluation stage of the paradigm, a large part of the screen had no relevance to the participant. Therefore, analysis was restricted to two regions of interest – the product region of interest (ROI) and the value scale ROI (green shaded area of Figure 3A-B). The fixation data, comprised of number of fixations per histogram bin, across the whole of each ROI were then submitted to a 3 (WTP categories) * 2 (free vs. forced) * 5 (time bins) repeated measures ANOVA to investigate the differences in fixation location between conditions. Given the large number of analyses from computing a three-way ANOVA on each histogram bin, P values were corrected using the Bonferroni-Holm (Holm, 1979) correction for multiple comparisons. Figure 3 summarises the results of all main effects. Firstly, three clusters of differences were observed across the product ROI, all indicating a significantly increased number of fixations for high value products. Secondly, a small cluster of significant differences was found on the left side of the value ROI, indicating an increased number of fixations for low value products. Thirdly, the cluster of significant differences indicated an increased number of fixations on the product ROI during forced bid trials, as well as an increased number of fixations on the value scale ROI during forced bid trials. Lastly, participants fixated progressively less on the product ROI and more so on the value scale ROI. Interaction effects did not indicate significant modulation and therefore did not require further investigation.

The same 40*40 bivariate histogram illustrating statistically significant differences between conditions was calculated with fixation duration parameters across the product and value scale ROI (Figure 4). Two major differences are observed between the number of fixations and corresponding fixation durations. Firstly, an increased number of fixations across the product ROI for high value products was paired with irregular differences in fixation duration. This suggests an increased number of fixations for high value products, independent of fixation duration, due to sporadic differences in fixation duration but a systematic increase in number of fixations. Secondly, an increased number of fixations on the product ROI during forced bid trials is paired with longer fixation durations during free bid trials on the product ROI. Hence, free bid trials elicited fewer but longer fixations, in contrast to forced bid trials eliciting many short fixations.

To further explore fixation data within the value scale ROI, fixations were extracted for each condition and the location of the fixations along the x-axis of the computer screen were normalised between -1 and 1. Transforming the time axis allowed for the visualisation of what set of values were being fixated during each time bin for each value category and trial type. Figure 5A demonstrates in the form of a bar graph how individuals were fixating in the centre of the value scale ROI regardless of value condition during TB1 for free bids. Fixating the centre of the screen during the initial viewing period was likely related to the indication of the type of condition (free vs forced) at this spot. However, in free bids, fixation location during TB2 was already predictive regarding low value items, with fixation location predicting their bid from TB3 onwards. This bias towards the left of the screen was reflected in the subjective WTP values in which the mean WTP for low and medium value items fall below the middle value of the scale. Figure 5B illustrates fixation locations during each time bin and each value category for forced bid trials, though no significant relationships were found.

3.3. Eye-fixation related potentials

ICs were clustered into 18 clusters. To identify the most significant clusters, confidence intervals were computed across the waveform for each cluster. To be submitted for further analysis, 95% confidence intervals had to exceed zero at peak component amplitude. This check resulted in nine clusters being submitted for further analysis. Mean component amplitude across the whole time course and IC maps are summarised in Figure 6. The number of components, as well as the number of subjects included in the cluster, are also reported.

The data from each of the nine clusters were submitted to a permutation-based repeated-measures ANOVA utilising 2500 permutations. Analysis was constrained to latencies between 50 ms and 270 ms to limit analysis to the latencies of brain potentials known to be involved in economic decisions (Tyson-Carr et al., 2018). A single cluster could contain a varying number of components belonging to different subjects, with subjects not necessarily contributing an equal number of components to any one cluster. Therefore, components belonging to the same subject were summated to produce a single component for each subject thus allowing for the preservation of the original null hypothesis. Consequently, statistical analysis on IC amplitude is in terms of summated component amplitude.

Firstly, an ANOVA with value category and trial type as independent variables was carried out to highlight the influence of these two factors on IC amplitude, either individually or interactively. Secondly, to investigate the interaction between value category and time bin, an ANOVA with value category and time bin as independent variables was carried out. Lastly, trial type and time bin were submitted to an ANOVA to investigate the interaction between these two variables. This resulted in a set of significant latencies for each cluster illustrating one of the above effects. Our method of permutation testing was limited to two factors which produced overlapping factors between the three ANOVAs completed. Hence, these permutation tests were used to detect latencies of interest across the clusters. Following extraction of these significant latencies, the corresponding omnibus ANOVA was completed to ensure the results were robust to the appropriate statistical tests.

In order to further restrict analyses, significant latencies were excluded based on two criteria. Firstly, significant differences had to be observed for a minimum of 5 consecutive milliseconds to ensure that the differences were not the result of momentary spikes. Next, latencies demonstrating significant interactions were excluded if the cluster did not first demonstrate a main effect within one of the independent variables. Results are summarised in Figures 7A-C.

Figure 7A highlights all significant latencies that demonstrated a significant main effect of value category across clusters. A significant effect of value was revealed between 158 and 165 ms in IC1, $F(2,34) = 3.46$, $P = .046$, $\eta_p^2 = .17$. High value items produced significantly decreased amplitude in comparison to both low value items, t(17) = 2.26, P = .033, *d* = 0.57, and medium value items, t(17) = 2.58, P = 0.02, *d* = 0.65. Separation of value categories was also observed for IC2 between 50 and 70 ms, F(2,34) = 6.49, P = .004, η_p^2 = .28, in which significantly increased amplitude was demonstrated for high value items in comparison to low value items, t(17) = 3.7, P < .001, *d* = 0.56, and medium value items, t(17) = 2.5, P = .024, *d* = 0.5. A similar effect was also demonstrated in IC3 between 148 and 160 ms, F(2,32) = 3.97, P = .028, η_p^2 = .2, with medium value items eliciting greater activity in comparison to low value items, t(16) = 2.34, P = .037, *d* = 0.61, and high value items, t(16) = 2.076, P = .041, *d* = 0.43. However, the component was at its strongest over a fronto-central region of the scalp. A statistically significant effect was revealed between 85 and 103 ms for IC4, F(2,34) = 3.42, P = .044, η_p^2 = .167, with high value items eliciting significantly increased amplitude in comparison to low value items, t(17) = 2.78, P = .015, *d* = 0.43. A second statistically significant effect of value in IC4 was revealed between 155 and 214 ms, F(2,34) = 3.7, P = .035, η_p^2 = .178. Post-hoc testing revealed significantly increased amplitude for medium value items in comparison to low value items, t(17) = 3.06, P = .004, *d* = 0.42.

Figure 7B demonstrates the main effects of trial type (free vs. forced bids). Three of the clusters demonstrated significantly increased activation during free bid trials. This effect was observed between 190 and 195 ms for IC1, F(1,17) = 5.06, P = .038, η_p^2 = .23, between 172 and 179 ms for IC2, F(1,17) = 4.72, P = .044, η_p^2 = .22, and lastly between 100 and 110 ms for IC5, F(1,16) = 4.9, P = .041, η_p^2 = .23. In contrast, two clusters demonstrated significantly increased activation during forced bid trials, firstly between 97 and 105 ms in IC4, F(1,17) = 4.9, P = .04, η_p^2 = .22, and also between 126 and 144 ms in IC6, F(1,17) = 11.8, P = .003, η_p^2 = .41.

As shown in Figure 7A, three significant effects separate different value categories. We therefore show in Figure 7C the corresponding time course of these activations across the 5 time bins in the same latencies. A main effect of time bin was observed for IC1 between 158 and 165 ms, $F(4,68) = 8.02$, $P < .001$, $\eta_p^2 = .32$. Post-hoc testing revealed significantly increased activation in TB1 in comparison to TB2, $t(17) = 4.66$, $P < .001$, $d = 1.25$, TB3, $t(17) = 4.95$, $P < 0.001$, $d = 1.47$, TB4, $t(17) = 4.39$, $P < 0.001$, $d = 1.37$, and TB5, $t(17) = 3.43$, $P = 0.007$, $d = 0.91$. For IC2 between 50 and 70 ms, no significant differences between time bins were found. A statistically significant effect of time bin was found for IC3 between 148 and 160 ms, $F(4,64) = 3.1$, $P = .021$, $\eta_p^2 = .16$. Post-hoc tests revealed significantly increased amplitude in TB1 in comparison to TB2, $t(16) = 2.34$, $P = 0.03$, $d = 0.81$, TB4, $t(16) = 2.78$, $P = 0.013$, $d = 0.91$, and TB5, $t(16) = 2.77$, $P = 0.014$, $d = 0.82$. It therefore appears that for clusters encoding low and medium value, activity is greatest early on during valuation, whereas it is maintained throughout the viewing period for high value brain components.

The interactions between value category and trial type are reported in Figure 7D. Here, only one significant effect was found for IC4 at a latency between 180 and 190 ms, $F(2,34) = 3.5$, $P = .041$, $\eta_p^2 = .17$. Following on from the main effect of value at a similar latency, this interaction appears to be a result of decreased amplitude for low value items in comparison to medium value items, $t(17) = 3.54$, $P = .002$, $d = 0.75$, and high value items, $t(17) = 2.7$, $P = .012$, $d = 0.51$, in the forced bid trials only.

Finally, the interactions between value and time bin are reported in Figure 7E. The only statistically significant interaction was found in IC2 in the epoch of 150 and 160 ms, $F(8,136) = 2.2$, $P = .035$, $\eta_p^2 = .11$. Post-hoc tests revealed significant differences in TB2, TB3 and TB4. In TB2, high value items elicited significantly increased amplitude in comparison to low value items, t(17) = 2.19, P = .017, *d* = 0.84. In TB3, medium values elicited increased amplitude in comparison to high value items, t(17) = 2.35, P = .028, *d* = 0.75. Finally, in TB4, high value items elicited significantly increased amplitude in comparison to low value items, t(17) = 2.1, P = 0.048, *d* = 0.74.

Since stimulus onset may have an influence on eye-fixation related potentials in the first time bin (Dimigen et al., 2011; Nikolaev et al., 2016), we carried out further analysis to account for any confounds. Firstly, we calculated the global field power based on the original grand average EFRP for each time bin and subject. Secondly, we averaged data across four separate latencies to summarise activity at the latency of the P1, P2, N2 and P3 components. Finally, we submitted this data to separate ANOVAs to determine whether the average amplitude of the corresponding components was influenced by time bin. Significant main effects of time bin were revealed for the P1 measured between 50 and 120 ms, $F(4,68) = 8.46$, $P < .001$, $\eta_p^2 = .33$, the P2 between 150 and 200 ms, $F(4,68) = 18.9$, $P < .001$, $\eta_p^2 = .53$, the N2 between 200 and 280 ms, $F(4,68) = 21.3$, $P < .001$, $\eta_p^2 = .56$, and the P3 between 280 and 350 ms, $F(4,68) = 23$, $P < .001$, $\eta_p^2 =.57$. All post-hoc tests revealed differences between time bin 1 and all other time bins ($P < .05$), with no other differences being present ($P \geq .05$). This suggests stimulus onset had a significant influence on the grand average EFRPs, and therefore, this may explain the differences observed between time bins in IC1 between 158 and 165 ms, and also between time bins in IC3 between 148 and 160 ms. However, the lack of differences between time bins in IC2 between 50 and 70 ms implies that this cluster is not influenced by stimulus onset, and therefore, may represent value-related activity.

Lastly, although EFRPs have been shown to be modulated by fixation rank (Fischer et al., 2013; Kamienkowski et al., 2018), the absence of differences between time bins after time bin 1 suggests brain data is not modulated by fixation rank in the current study.

4. Discussion

The present study postulated the presence of value-specific cortical activation components of which at least some would respond to a specific value category early on during the viewing period and maintain their activations throughout the viewing period both during free and forced bid trials. The findings largely support our predictions. Firstly, unique cortical activation components were observed for high, medium and low/medium value products. Additionally, a left, middle, right lateralisation effect was found for high, medium, low/medium value products, respectively. Secondly, effects were mostly observed within the latency of the N2 EEG component, emphasising the importance of this component in economic valuation processing. Lastly, the brain component specific to high value did not significantly vary throughout the valuation stage. The maintained component activation for high value products suggests the increased cognitive processing required for high value items in comparison to low and medium value items. The fixation heat maps indicating an increased number of fixations, independent of fixation duration, across the product for high value products provides further support for this increased cognitive processing, similar to previous studies (Anderson and Halpern, 2017; Anderson and Yantis, 2012).

Brain components encoding distinct categories of stimuli is prevalent across many domains. For example, the N170 EEG component has frequently been described as being an activation specific to face-processing (Calvo and Beltran, 2013; Cao et al., 2014; Zhang et al., 2013), as well as encoding the emotional valence of faces (Qiu et al., 2017). Evidence for the encoding of emotional valence is also prevalent amongst several other brain components. For example, the P1, N1, P2 and N2 components have been shown to respond to stimuli with a negative valence (Huang and Luo, 2006; Lithari et al., 2010; Smith et al., 2003). It has also been demonstrated that the encoding of negative valence can persist into later components such as the LPP (Schupp et al., 2004). Lithari et al. (2010) highlighted the role of the P3 component in the encoding of positive valence, however, also emphasised the role of the P2 component in positive valence encoding. A rapid categorisation of stimuli according to their economic value may encourage fast responses offering the best possible decision outcome (Brosch et al., 2010). Results suggest a rapid and approximate categorisation of stimuli according to their subjective values in which low and high value items are clearly differentiated. Interestingly, a separate scalp pattern was associated with medium value products. The presence of a specific component featuring activation over the midline scalp regions may be a result of absence of either the left-hemisphere high-value or the right-hemisphere low-value value allocation.

Further to the categorisation of subjective value, lateralisation of cortical activation was also observed. IC2, which distinguished the processing of high value items, was most prominent over the left parietal region of the scalp, whereas IC1 demonstrated a spatial maximum that extended over a right frontal region of the scalp and responded to low/medium value products. Hemispheric asymmetry regarding the role of the left and right hemispheres, and their relatedness to approach and withdrawal behaviours respectively, has long been established (see Hakim and Levy, 2019). Similarly, this asymmetry has been observed concerning emotions, motivation and affect (Davidson, 1998; Demaree et al., 2005; Harmon-Jones et al., 2010). The affective valence hypothesis (Alves et al., 2008) and previous studies (Lawrence et al., 2012; Price and Harmon-Jones, 2011) also highlight the role of the left hemisphere in approach behaviour.

In the ERP domain, Aguado et al. (2013) reported an increase in LPP amplitude over left temporal regions for positive facial expressions – also, the encoding of negative affect in the right hemisphere has been frequently observed (Ahern and Schwartz, 1985; Balconi and Mazza, 2009; Kokmotou et al., 2017; Windmann et al., 2006). Additionally, a left/right hemispheric lateralisation during the evaluation of pleasant/unpleasant odours has been reported (Cook et al., 2015; Henkin and Levy, 2001). Critically, Pizzagalli et al. (2005) link approach behaviour with the evaluation of rewards allowing us to speculate on hemispheric asymmetry in terms of valuation processes. In the time-frequency domain, increased slow-wave oscillations originating from the right prefrontal cortex were indicative of an increased inclination for risk (Gianotti et al., 2009). From a neuromarketing perspective, Ohme et al. (2010) posited that frontal asymmetry might be an important tool for evaluating the effectiveness of adverts. Further evidence for this comes from the increase of theta and alpha activity in the left and right hemisphere whilst observing pleasant and unpleasant adverts respectively (Vecchiato et al., 2014; Vecchiato et al., 2011).

The present finding of left frontal activations, represented by IC2, is in line with the valence hypothesis and suggest that goods with high economic value may share the same neural representation as positive affect and could possibly be indicative of motivation related processes, specifically approach behaviours. It could be argued that in a similar fashion to the bias towards low value items (Tyson-Carr et al., 2018), low value stimuli could induce withdrawal behaviours due to being potential sources of financial loss. For example, Shenhav et al. (2018) reported that choosing between low value items could induce anxiety since these items can be interpreted as aversive in certain situations.

From a functional brain imaging perspective, brain regions encoding value either positively or negatively have been reported (Bartra et al., 2013). In their meta-analysis, Bartra et al. pointed out that several brain regions demonstrated either positive or negative encoding of value, or even both positive and negative encoding together. Anatomically, the OFC specifically has been subject to a volume of research regarding the functions of its sub-regions. The discrimination of the lateral and medial aspects of the OFC is well documented (Kringelbach and Rolls, 2004; Zald et al., 2014), and even finer organisations have been suggested (Kahnt et al., 2012; Mackey and Petrides, 2010; Ongur et al., 2003). The distinct functional connectivity of multiple sub-regions demonstrates the ability of the OFC to encode a wide variety of values, such as both reward and punishment (Elliott et al., 2000; O'Doherty et al., 2001), making it a candidate for the encoding of distinct value categories. Our data suggests that the valuation process occurring during free viewing of goods is based on sets of activation patterns which are employed in response to either low, medium or high value but none of these patterns encodes the value throughout the whole range of values.

A benefit of analysing cortical responses to individual successive eye fixations is the ability to highlight value encoding across the time course of a decision. A single interaction between value and time bin within IC2 is characterised by differences within TB2, TB3 and TB4, with the most linear encoding of value present in TB2. As is emphasised by the fixation location data, it was as early as 800-1600 ms post stimulus onset when individuals have most likely already decided the amount they are ultimately willing to bid. IC strength was also highest in this time bin for high value items, reiterating the link between this cluster and the valuation of high value products. However, an important finding was the activation cluster observed over subsequent time bins, specifically for the ICs that decode different value categories. The brain component encoding high value showed no significant variation throughout the time course, although confidence intervals did overlap with zero in the third time bin, suggesting the increased amount of cognitive processing that takes place when valuating high value options.

The reported fixation heat maps showed an increased number of fixations for high value items. This greater number of fixations is an indicator of an increased amount of time spent valuating the product and provides evidence for an increased amount of cognitive resources utilised during the valuation of high value products, something that has been observed in previous studies (Audrin et al., 2018; McGinty et al., 2016; Simola et al., 2015). A wealth of research has highlighted how the emotional content of a scene can modulate the nature of eye-fixations. A previous study demonstrated increased attention towards both positive and negative stimuli, reflected in longer fixation durations and more rapid fixation onsets (Nummenmaa et al., 2006). Similarly, eye-movements are more likely to be directed towards scenes that are affectively salient in comparison to scenes that are simply visually salient (Niu et al., 2012). Various eye-movement characteristics have also been shown to predict scene valence (Tavakoli et al., 2015) and eye-tracking can be used to infer cognitive processes such as attention (Hayhoe and Ballard, 2005). From an economic decision making perspective, we are more likely to choose items that we fixate for longer (Cisek et al., 2014; McGinty et al., 2016), which is especially true for luxury products (Audrin et al., 2018). A study by Simola et al. (2015) reported enhanced fixation rates and longer gaze durations for unpleasant stimuli when they also had high arousal. However, gaze duration and fixation rates were increased for pleasant stimuli when they had low arousal. The increased number of fixations for high value products in the current study, as demonstrated in the fixation heat maps, may reflect the same processes as reported in this previous study by Simola et al., whereby the high value products are pleasant but not arousing, thus eliciting a larger number of fixations. Conversely, the fixation heat maps also demonstrate an increased number of fixations on the value scale for low value products, indicating that the value of low value products was decided rapidly and fixating on the product was no longer necessary given this quick categorisation.

Our data are relevant for evaluation of the drift-diffusion models of the valuation processing resting on accumulation of evidence during decision making tasks. Drift-diffusion models have been utilised to explain choices during binary decisions (Krajbich et al., 2010), trinary decisions (Krajbich and Rangel, 2011) and simple purchase decisions (Krajbich et al., 2012). Milosavljevic et al. (2010) employed the drift-diffusion model to demonstrate a fast, under 1000 ms, elaboration of decision value by accumulation of noisy information until a decision threshold is reached. Using single neuron recordings, much of this research revealed the role of the OFC, the lateral prefrontal cortex and the anterior cingulate cortex in value encoding in animals (Padoa-Schioppa, 2009; Padoa-Schioppa and Assad, 2006; Tremblay and Schultz, 1999; Wallis and Miller, 2003), with value differentiation observed at approximately 450 ms post stimulus (Kennerley et al., 2009). Single neuron recordings in humans have also revealed the role of the amygdala in value encoding, and importantly, how the neuronal spike count differentiated value as early as 250 ms (Jenison et al., 2011). ERP methods have also reiterated this and revealed rapid value encoding in the brain (Larsen and O'Doherty, 2014), even as early as 150 ms (Harris et al., 2011). Our results point to a rapid categorisation of stimuli according to their economic values occurring within an epoch comprising two 800-ms time bins and this finding is consistent with both the drift-diffusion model data (Milosavljevic et al., 2010) and single-neuron studies in animals.

The automaticity of the valuation process was captured in the differences between forced and free bids. Forced bidding trials allowed for the disentanglement of valuation specific processes from generic, non-specific neural processes (Plassmann et al., 2007, 2010). IC1, IC2 and IC5 each demonstrated increased strength for free bids. It would, therefore, seem that brain component expressed in IC1 is responsible for the encoding of low value products, and IC2 for high value products, most prominently in free bidding procedures. IC5, though showing no segregation of value, is specific to deliberate valuation. IC4, a component that was reported to be unique to medium/high value items in the forced bidding condition, demonstrated increased strength during forced bidding along with IC6. The presence of an automatic valuation system in the brain has previously been demonstrated in which value appeared to be computed in value-irrelevant tasks (Grueschow et al., 2015; Lebreton et al., 2009). There is also a wealth of research investigating value-driven attentional capture, the process whereby value is used as a cue to capture attention, which highlights the automatic nature of valuation processes. For example, the presence of a distractor in a binary decision task will increase reaction times and reduce decision optimality as the learned value of the distractor increases (Itthipuripat et al., 2015). Additionally, attention and eyes were captured during unconstrained viewing by task-irrelevant but previously rewarded stimuli (Anderson and Yantis, 2012), thus emphasising the ability to automatically evaluate stimuli within our visual field despite their lack of relevance to the current task.

An important consideration when using simultaneous EEG and eye-tracking recordings is the potential influence of eye-movement characteristics on EEG components. The SP, a potential observed at saccade onset, is modulated by saccade sizes and direction (Keren et al., 2010), and the visual lambda response can be modulated by fixation duration and saccade sizes (Nikolaev et al., 2016). In the present study, the varying temporal overlap between fixation events suggests that some effects could be explained by eye-movement related events alone. However, this is an inherent condition of free-viewing situations and several methods can be used to control for these factors. For example, we utilise here the method of linear deconvolution, using Unfold (Ehinger and Dimigen, 2018), to confirm our independent component clusters. Using this method, we revealed that saccade initiation was not likely to have had an influence on the cluster waveforms.

Traditional ERP experimental designs limit understanding to the initial cognitive processing that takes place within the first second following stimulus onset. However, although evidence suggests that value encoding occurs rapidly (Harris et al., 2011; Roberts et al., 2018; Tyson-Carr et al., 2018), further deliberation over time may influence the final evaluation. Past research indeed highlights how value-based decisions are guided by evidence accumulation until a decision point is ultimately reached (Krajbich et al., 2010; Krajbich et al., 2012; Krajbich and Rangel, 2011; Polania et al., 2014). Importantly, Melcher and Colby (2008) highlight in their framework how information between subsequent saccades is integrated to produce a more complex view of the world and it is this sequential remapping of sensory information that we speculate could underpin value-guided choice. It is these trans-saccadic processes that are of great relevance to the growing field of real-world neuroimaging. In real life, our conscious experience comprises a series of fixations to gather information and initiate motor behaviours. Not only can we disentangle the trans-saccadic gathering of information, the method also benefits from the outstanding temporal resolution of EEG, something which fMRI methods severely lack. The method described in this study is also easily applicable to real life settings to help further our understanding of value-guided choice in a naturalistic setting (Roberts et al., 2018; Soto et al., 2018). A well-known drawback of this method is the contamination of EEG data with saccades. Any systematic difference in eye-movements between conditions can easily produce false-positives. However, recent advanced methods of analysis of eye fixation related potentials, such as the Unfold toolbox (Ehinger and Dimigen, 2018), can account for a large proportion of the confounds that eye-movements can introduce.

The present study aimed to reveal the brain components responsible for valuating specific value categories in the context of EEG. However, the treatment of WTP as a continuous factor may reveal, more generally, the dynamics of economic valuation in the brain. Future research would benefit from revealing correlations of brain components with WTP to emphasise the temporal characteristics of a more general subjective valuation system. A final consideration is the minimum effect duration in the current study. The current study implemented a minimum duration of 5 ms for effects to be interpreted. Although this avoids interpreting effects resulting from momentary differences spanning a few samples, it is uncertain to what extent differences being observed for 5 ms may reflect higher-order cognitive processes.

To conclude, we demonstrate for the first time that valuation processes can be tracked over the time course of a decision using combined eye-tracking and EEG recordings. Our study advances the knowledge of temporal dynamics of the valuation process which has been acquired using event-related potentials locked to the onset of fixations. A set of brain components were revealed that encoded distinct value categories, each with a unique presentation across the scalp that reiterated the encoding of positive and negative affect in the left and right hemispheres respectively. Value categorisation for products is achieved automatically as it also occurred during forced bid choices and economic valuation appears to be largely completed within 1600 ms after presenting a visual stimulus.

Acknowledgements

This work was supported by a CASE studentship from the Economic and Social Research Council [grant number ES/J500094/1], with additional support from Unilever Research and Development.

Figure Legends

Figure 1 A timeline of the main auction task. A fixation cross was presented for 2 s followed by image presentation for 4 s, during which the trial type is indicated. If a '?' is presented below the image, individuals are allowed to bid freely after the image has offset. If a monetary amount is shown instead, the individuals must bid the reported amount. Following bidding, feedback was presented for 1 s to indicate the auction outcome.

Figure 2 95% HPD confidence intervals for saccade direction measured in degrees of visual angle for each condition.

Figure 3 Fixation locations. Heatmaps indicating fixation location differences within conditions for the image region (A; green highlighted area) and the scale region (B; green highlighted area). Bar graphs showing mean number of fixations per histogram bin. Bar graphs also indicate direction of effects for each cluster of differences.

Figure 4 Fixation durations. Heatmaps indicating fixation duration differences within conditions for the image region (A; green highlighted area) and the scale region (B; green highlighted area). Bar graphs showing mean fixation duration in each histogram bin. Bar graphs also indicate direction of effects for each cluster of differences.

Figure 5 Scale fixations x-axis coordinates. Mean x-axis coordinates for fixations on the scale normalised between -1 and 1. Mean coordinates for each value category and time bin are shown for free bids (A) and forced bids (B). Post-hoc tests are shown: * = $P < .05$, ** = $P < .01$, *** = $P < .001$.

Figure 6 EFRP clusters. Independent component clusters for EFRP data that passed confidence intervals checks are illustrated with their corresponding waveforms and scalp maps. Time scales of IC waveforms are measured in ms.

Figure 7 EFRP cluster effects. Clusters that demonstrate main effects of value category (A) or trial type (B) are shown, along with the time course of activations for the value relevant effects in IC1, IC2 and IC3 with corresponding effects (C). An interaction between value category and trial type (D) and an interaction between value category and time bin (E) are also illustrated. Time scales of IC waveforms are measured in ms.

References

Aguado, L., Dieguez-Risco, T., Mendez-Bertolo, C., Pozo, M.A., Hinojosa, J.A., 2013. Priming effects on the N400 in the affective priming paradigm with facial expressions of emotion. Cogn Affect Behav Neurosci 13, 284-296. https://doi.org/10.3758/s13415-012-0137-3

Ahern, G.L., Schwartz, G.E., 1985. Differential lateralization for positive and negative emotion in the human brain: EEG spectral analysis. Neuropsychologia 23, 745-755

Alves, N.T., Fukusima, S.S., Aznar-Casanova, J.A., 2008. Models of brain asymmetry in emotional processing. Psychology & Neuroscience 1, 63-66. https://doi.org/10.3922/j.psns.2008.1.010

Anderson, B.A., Halpern, M., 2017. On the value-dependence of value-driven attentional capture. Atten Percept Psychophys 79, 1001-1011. https://doi.org/10.3758/s13414-017-1289-6

Anderson, B.A., Yantis, S., 2012. Value-driven attentional and oculomotor capture during goal-directed, unconstrained viewing. Atten Percept Psychophys 74, 1644-1653. https://doi.org/10.3758/s13414-012-0348-2

Audrin, C., Brosch, T., Sander, D., Chanal, J., 2018. More than meets the eye: The impact of materialism on information selection during luxury choices. Front Behav Neurosci 12, 172. https://doi.org/10.3389/fnbeh.2018.00172

Baccino, T., Manunta, Y., 2005. Eye-fixation-related potentials: Insight into parafoveal processing. Journal of Psychophysiology 19, 204-215. https://doi.org/10.1027/0269-8803.19.3.204

Balconi, M., Mazza, G., 2009. Brain oscillations and BIS/BAS (behavioral inhibition/activation system) effects on processing masked emotional cues.

ERS/ERD and coherence measures of alpha band. Int J Psychophysiol 74, 158-165. https://doi.org/10.1016/j.ijpsycho.2009.08.006

Bartra, O., McGuire, J.T., Kable, J.W., 2013. The valuation system: a coordinate-based meta-analysis of BOLD fMRI experiments examining neural correlates of subjective value. Neuroimage 76, 412-427. https://doi.org/10.1016/j.neuroimage.2013.02.063

Becker, G., Degroot, M., Marschak, J., 1964. Measuring utility by a single-response sequential method. Behavioral Science 9, 226-232

Berens, P., 2009. CircStat: A MATLAB toolbox for circular statistics. Journal of Statistical Software 31, 1-21

Berg, P., Scherg, M., 1994. A multiple source approach to the correction of eye artifacts. Electroencephalography and Clinical Neurophysiology 90, 229-241

Blignaut, P., 2009. Fixation identification: the optimum threshold for a dispersion algorithm. Atten Percept Psychophys 71, 881-895. https://doi.org/10.3758/APP.71.4.881

Boylan, C., Doig, H.R., 1989. Effect of saccade size on presaccadic spike potential amplitude. Investigative Ophthalmology & Visual Science 30, 2521-2527

Brosch, T., Pourtois, G., Sander, D., 2010. The perception and categorisation of emotional stimuli: A review. Cognition & Emotion 24, 377-400. https://doi.org/10.1080/02699930902975754

Calvo, M.G., Beltran, D., 2013. Recognition advantage of happy faces: tracing the neurocognitive processes. Neuropsychologia 51, 2051-2061. https://doi.org/10.1016/j.neuropsychologia.2013.07.010

Cao, X., Jiang, B., Gaspar, C., Li, C., 2014. The overlap of neural selectivity between faces and words: evidences from the N170 adaptation effect. Exp Brain Res 232, 3015-3021. https://doi.org/10.1007/s00221-014-3986-x

Chib, V.S., Rangel, A., Shimojo, S., O'Doherty, J.P., 2009. Evidence for a common representation of decision values for dissimilar goods in human ventromedial prefrontal cortex. J Neurosci 29, 12315-12320. https://doi.org/10.1523/JNEUROSCI.2575-09.2009

Cisek, S.Z., Sedikides, C., Hart, C.M., Godwin, H.J., Benson, V., Liversedge, S.P., 2014. Narcissism and consumer behaviour: a review and preliminary findings. Front Psychol 5, 232. https://doi.org/10.3389/fpsyg.2014.00232

Clithero, J.A., Rangel, A., 2014. Informatic parcellation of the network involved in the computation of subjective value. Soc Cogn Affect Neurosci 9, 1289-1302. https://doi.org/10.1093/scan/nst106

Cook, S., Fallon, N., Wright, H., Thomas, A., Giesbrecht, T., Field, M., Stancak, A., 2015. Pleasant and unpleasant odors influence hedonic evaluations of human faces: An event-related potential study. Front Hum Neurosci 9, 661. https://doi.org/10.3389/fnhum.2015.00661

Cremers, J., Klugkist, I., 2018. One direction? A tutorial for circular data analysis using R with examples in cognitive psychology. Frontiers in Psychology 9. https://doi.org/10.3389/fpsyg.2018.02040

Davidson, R.J., 1998. Anterior electrophysiological asymmetries, emotion, and depression: Conceptual and methodological conundrums. Psychophysiology 35, 607-614

Delorme, A., Makeig, S., 2004. EEGLAB: an open source toolbox for analysis of single-trial EEG dynamics including independent component analysis. J Neurosci Methods 134, 9-21. https://doi.org/10.1016/j.jneumeth.2003.10.009

Demaree, H.A., Everhart, D.E., Youngstrom, E.A., Harrison, D.W., 2005. Brain lateralization of emotional processing: Historical roots and a future incorporating "dominance". Behav Cogn Neurosci Rev 4, 3-20. https://doi.org/10.1177/1534582305276837

Dimigen, O., Sommer, W., Hohlfeld, A., Jacobs, A.M., Kliegl, R., 2011. Coregistration of eye movements and EEG in natural reading: analyses and review. J Exp Psychol Gen 140, 552-572. https://doi.org/10.1037/a0023885

Ehinger, B.V., Dimigen, O., 2018. Unfold: An integrated toolbox for overlap correction, non-linear modeling, and regression-based EEG analysis. https://doi.org/10.1101/360156

Elliott, R., Dolan, R.J., Frith, C.D., 2000. Dissociable functions in the medial and lateral orbitofrontal cortex: Evidence from human neuroimaging studies. Cereb Cortex 10

Fischer, T., Graupner, S.T., Velichkovsky, B.M., Pannasch, S., 2013. Attentional dynamics during free picture viewing: Evidence from oculomotor behavior and electrocortical activity. Front Syst Neurosci 7, 17. https://doi.org/10.3389/fnsys.2013.00017

Gehring, W.J., Liu, Y., Orr, J.M., Carp, J., 2012. The Error-Related Negativity (ERN/Ne). In: Luck, S.J., Kappenman, E.S. (Eds.), The Oxford Handbook of Event-Related Potential Components

Gianotti, L.R.R., Knoch, D., Faber, P.L., Lehmann, D., Pascual-Marqui, R.D., Diezi, C., Schoch, C., Eisenegger, C., Fehr, E., 2009. Tonic activity level in the right prefrontal cortex predicts individuals' risk taking. Psychological Science 20, 33-38

Glimcher, P.W., Fehr, E., 2014. Neuroeconomics: Decsion making and the brain. Elsevier Academic Press

Grueschow, M., Polania, R., Hare, T.A., Ruff, C.C., 2015. Automatic versus choice-dependent value representations in the human brain. Neuron 85, 874-885. https://doi.org/10.1016/j.neuron.2014.12.054

Hakim, A., Levy, D.J., 2019. A gateway to consumers' minds: Achievements, caveats, and prospects of electroencephalography-based prediction in neuromarketing. Wiley Interdiscip Rev Cogn Sci 10, e1485. https://doi.org/10.1002/wcs.1485

Hare, T.A., O'Doherty, J., Camerer, C.F., Schultz, W., Rangel, A., 2008. Dissociating the role of the orbitofrontal cortex and the striatum in the computation of goal values and prediction errors. J Neurosci 28, 5623-5630. https://doi.org/10.1523/JNEUROSCI.1309-08.2008

Harmon-Jones, E., Gable, P.A., Peterson, C.K., 2010. The role of asymmetric frontal cortical activity in emotion-related phenomena: A review and update. Biol Psychol 84, 451-462. https://doi.org/10.1016/j.biopsycho.2009.08.010

Harris, A., Adolphs, R., Camerer, C., Rangel, A., 2011. Dynamic construction of stimulus values in the ventromedial prefrontal cortex. PLoS One 6, e21074. https://doi.org/10.1371/journal.pone.0021074

Hayhoe, M., Ballard, D., 2005. Eye movements in natural behavior. Trends Cogn Sci 9, 188-194. https://doi.org/10.1016/j.tics.2005.02.009

Henkin, R.I., Levy, L.M., 2001. Lateralization of brain activation to imagination and smell of odors using functional magnetic resonance imaging (fMRI): Left hemispheric localization of pleasant and right hemispheric localization of unpleasant odors. Journal of Computer Assisted Tomography 25, 493-514. https://doi.org/10.1097/00004728-200107000-00001

Holm, S., 1979. A simple sequentially rejective multiple test procedure. Scandinavian Journal of Statistics 6, 65-70

Huang, Y.X., Luo, Y.J., 2006. Temporal course of emotional negativity bias: An ERP study. Neurosci Lett 398, 91-96. https://doi.org/10.1016/j.neulet.2005.12.074

Hunt, L.T., Kolling, N., Soltani, A., Woolrich, M.W., Rushworth, M.F., Behrens, T.E., 2012. Mechanisms underlying cortical activity during value-guided choice. Nat Neurosci 15, 470-476, S471-473. https://doi.org/10.1038/nn.3017

Hutzler, F., Braun, M., Vo, M.L., Engl, V., Hofmann, M., Dambacher, M., Leder, H., Jacobs, A.M., 2007. Welcome to the real world: Validating fixation-related brain potentials for ecologically valid settings. Brain Res 1172, 124-129. https://doi.org/10.1016/j.brainres.2007.07.025

Itthipuripat, S., Cha, K., Rangsipat, N., Serences, J.T., 2015. Value-based attentional capture influences context-dependent decision-making. J Neurophysiol 114, 560-569. https://doi.org/10.1152/jn.00343.2015

Jenison, R.L., Rangel, A., Oya, H., Kawasaki, H., Howard, M.A., 2011. Value encoding in single neurons in the human amygdala during decision making. J Neurosci 31, 331-338. https://doi.org/10.1523/JNEUROSCI.4461-10.2011

Kahnt, T., Chang, L.J., Park, S.Q., Heinzle, J., Haynes, J.D., 2012. Connectivity-based parcellation of the human orbitofrontal cortex. J Neurosci 32, 6240-6250. https://doi.org/10.1523/JNEUROSCI.0257-12.2012

Kamienkowski, J.E., Varatharajah, A., Sigman, M., Ison, M.J., 2018. Parsing a mental program: Fixation-related brain signatures of unitary operations and routines in natural visual search. Neuroimage 183, 73-86. https://doi.org/10.1016/j.neuroimage.2018.08.010

Kassner, M., Patera, W., Bulling, A., 2014. Pupil: An open source platform for pervasive eye tracking and mobile gaze-based interaction.

Kennerley, S.W., Dahmubed, A.F., Lara, A.H., Wallis, J.D., 2009. Neurons in the frontal lobe encode the value of multiple decision variables. J Cogn Neurosci 21, 1162-1178. https://doi.org/10.1162/jocn.2009.21100

Keren, A.S., Yuval-Greenberg, S., Deouell, L.Y., 2010. Saccadic spike potentials in gamma-band EEG: Characterization, detection and suppression. Neuroimage 49, 2248-2263. https://doi.org/10.1016/j.neuroimage.2009.10.057

Kiss, M., Driver, J., Eimer, M., 2009. Reward priority of visual target singletons modulates event-related potential signatures of attentional selection. Psychol Sci 20, 245-251. https://doi.org/10.1111/j.1467-9280.2009.02281.x

Kokmotou, K., Cook, S., Xie, Y., Wright, H., Soto, V., Fallon, N., Giesbrecht, T., Pantelous, A., Stancak, A., 2017. Effects of loss aversion on neural responses to loss outcomes: An event-related potential study. Biol Psychol 126, 30-40. https://doi.org/10.1016/j.biopsycho.2017.04.005

Krajbich, I., Armel, C., Rangel, A., 2010. Visual fixations and the computation and comparison of value in simple choice. Nat Neurosci 13, 1292-1298. https://doi.org/10.1038/nn.2635

Krajbich, I., Lu, D., Camerer, C., Rangel, A., 2012. The attentional drift-diffusion model extends to simple purchasing decisions. Front Psychol 3, 193. https://doi.org/10.3389/fpsyg.2012.00193

Krajbich, I., Rangel, A., 2011. Multialternative drift-diffusion model predicts the relationship between visual fixations and choice in value-based decisions. PNAS 108, 13852-13857

Kringelbach, M.L., Rolls, E.T., 2004. The functional neuroanatomy of the human orbitofrontal cortex: Evidence from neuroimaging and neuropsychology. Prog Neurobiol 72, 341-372. https://doi.org/10.1016/j.pneurobio.2004.03.006

Larsen, T., O'Doherty, J.P., 2014. Uncovering the spatio-temporal dynamics of value-based decision-making in the human brain: A combined fMRI-EEG study. Philos Trans R Soc Lond B Biol Sci 369. https://doi.org/10.1098/rstb.2013.0473

Lawrence, N.S., Hinton, E.C., Parkinson, J.A., Lawrence, A.D., 2012. Nucleus accumbens response to food cues predicts subsequent snack consumption in women and increased body mass index in those with reduced self-control. Neuroimage 63, 415-422. https://doi.org/10.1016/j.neuroimage.2012.06.070

Lebreton, M., Jorge, S., Michel, V., Thirion, B., Pessiglione, M., 2009. An automatic valuation system in the human brain: evidence from functional neuroimaging. Neuron 64, 431-439. https://doi.org/10.1016/j.neuron.2009.09.040

Lehmann, D., 1984. EEG assessment of brain activity: Spatial aspects, segmentation and imaging. International Journal of Psychophysiology 1, 267-276

Levy, D.J., Glimcher, P.W., 2012. The root of all value: A neural common currency for choice. Curr Opin Neurobiol 22, 1027-1038. https://doi.org/10.1016/j.conb.2012.06.001

Lithari, C., Frantzidis, C.A., Papadelis, C., Vivas, A.B., Klados, M.A., Kourtidou-Papadeli, C., Pappas, C., Ioannides, A.A., Bamidis, P.D., 2010. Are females more responsive to emotional stimuli? A neurophysiological study across arousal and valence dimensions. Brain Topogr 23, 27-40. https://doi.org/10.1007/s10548-009-0130-5

Luck, S.J., 2005. An introduction to the event-related potential technique. MIT Press, Cambridge, Mass

Mackey, S., Petrides, M., 2010. Quantitative demonstration of comparable architectonic areas within the ventromedial and lateral orbital frontal cortex in the human and the macaque monkey brains. Eur J Neurosci 32, 1940-1950. https://doi.org/10.1111/j.1460-9568.2010.07465.x

McGinty, V.B., Rangel, A., Newsome, W.T., 2016. Orbitofrontal cortex value signals depend on fixation location during free viewing. Neuron 90, 1299-1311. https://doi.org/10.1016/j.neuron.2016.04.045

Melcher, D., Colby, C.L., 2008. Trans-saccadic perception. Trends Cogn Sci 12, 466-473. https://doi.org/10.1016/j.tics.2008.09.003

Milosavljevic, M., Malmaud, J., Huth, A., Koch, C., Rangel, A., 2010. The Drift Diffusion Model can account for the accuracy and reaction time of value-based choices under high and low time pressure. Judgment and Decision Making 5

Nieuwenhuis, S., Holroyd, C.B., Mol, N., Coles, M.G., 2004. Reinforcement-related brain potentials from medial frontal cortex: Origins and functional significance. Neurosci Biobehav Rev 28, 441-448. https://doi.org/10.1016/j.neubiorev.2004.05.003

Nikolaev, A.R., Meghanathan, R.N., van Leeuwen, C., 2016. Combining EEG and eye movement recording in free viewing: Pitfalls and possibilities. Brain Cogn 107, 55-83. https://doi.org/10.1016/j.bandc.2016.06.004

Niu, Y., Todd, R.M., Anderson, A.K., 2012. Affective salience can reverse the effects of stimulus-driven salience on eye movements in complex scenes. Front Psychol 3, 336. https://doi.org/10.3389/fpsyg.2012.00336

Nummenmaa, L., Hyona, J., Calvo, M.G., 2006. Eye movement assessment of selective attentional capture by emotional pictures. Emotion 6, 257-268. https://doi.org/10.1037/1528-3542.6.2.257

O'Doherty, J., Kringelbach, M.L., Rolls, E.T., Hornak, J., Andrews, C., 2001. Abstract reward and punishment representations in the human orbitofrontal cortex. Nature Neuroscience 4, 95-102

Ohme, R., Reykowska, D., Wiener, D., Choromanska, A., 2010. Application of frontal EEG asymmetry to advertising research. Journal of Economic Psychology 31, 785-793. https://doi.org/10.1016/j.joep.2010.03.008

Ongur, D., Ferry, A.T., Price, J.L., 2003. Architectonic subdivision of the human orbital and medial prefrontal cortex. J Comp Neurol 460, 425-449. https://doi.org/10.1002/cne.10609

Padoa-Schioppa, C., 2009. Range-adapting representation of economic value in the orbitofrontal cortex. J Neurosci 29, 14004-14014. https://doi.org/10.1523/JNEUROSCI.3751-09.2009

Padoa-Schioppa, C., Assad, J.A., 2006. Neurons in the orbitofrontal cortex encode economic value. Nature 441, 223-226. https://doi.org/10.1038/nature04676

Peters, J., Buchel, C., 2010. Neural representations of subjective reward value. Behav Brain Res 213, 135-141. https://doi.org/10.1016/j.bbr.2010.04.031

Pizzagalli, D.A., Sherwood, R.J., Henriques, J.B., Davidson, R.J., 2005. Frontal brain asymmetry and reward responsiveness: A source-localization study. Psychological Science 16, 805-813

Plassmann, H., O'Doherty, J.P., Rangel, A., 2007. Orbitofrontal cortex encodes willingness to pay in everyday economic transactions. J Neurosci 27, 9984-9988. https://doi.org/10.1523/JNEUROSCI.2131-07.2007

Plassmann, H., O'Doherty, J.P., Rangel, A., 2010. Appetitive and aversive goal values are encoded in the medial orbitofrontal cortex at the time of decision making. J Neurosci 30, 10799-10808. https://doi.org/10.1523/JNEUROSCI.0788-10.2010

Polania, R., Krajbich, I., Grueschow, M., Ruff, C.C., 2014. Neural oscillations and synchronization differentially support evidence accumulation in perceptual and value-based decision making. Neuron 82, 709-720. https://doi.org/10.1016/j.neuron.2014.03.014

Price, T.F., Harmon-Jones, E., 2011. Approach motivational body postures lean toward left frontal brain activity. Psychophysiology 48, 718-722. https://doi.org/10.1111/j.1469-8986.2010.01127.x

Qiu, R., Wang, H., Fu, S., 2017. N170 Reveals the Categorical Perception Effect of Emotional Valence. Front Psychol 8, 2056. https://doi.org/10.3389/fpsyg.2017.02056

R Core Team, 2018. R: A language and environment for statistical computing. R Foundation for Statistical Computing, Vienna, Austria

Rangel, A., Camerer, C., Montague, P.R., 2008. A framework for studying the neurobiology of value-based decision making. Nat Rev Neurosci 9, 545-556. https://doi.org/10.1038/nrn2357

Riemslag, F.C.C., Van der Heijde, G.L., Van Dongen, M.M.M.M., Ottenhoff, F., 1988. On the origin of the presaccadic spike potential. Electroencephalography and Clinical Neurophysiology 70, 281-287

Roberts, H., Soto, V., Tyson-Carr, J., Kokmotou, K., Cook, S., Fallon, N., Giesbrecht, T., Stancak, A., 2018. Tracking economic value of products in natural settings: A wireless EEG study. Front Neurosci 12, 910. https://doi.org/10.3389/fnins.2018.00910

San Martin, R., 2012. Event-related potential studies of outcome processing and feedback-guided learning. Front Hum Neurosci 6, 304. https://doi.org/10.3389/fnhum.2012.00304

Schultz, W., 2017. Electrophysiological correlates of reward processing in dopamine neurons. Decision Neuroscience, pp. 21-31. https://doi.org/10.1016/b978-0-12-805308-9.00002-6

Schupp, H.T., Ohman, A., Junghofer, M., Weike, A.I., Stockburger, J., Hamm, A.O., 2004. The facilitated processing of threatening faces: an ERP analysis. Emotion 4, 189-200. https://doi.org/10.1037/1528-3542.4.2.189

Shenhav, A., Dean Wolf, C.K., Karmarkar, U.R., 2018. The evil of banality: When choosing between the mundane feels like choosing between the worst. J Exp Psychol Gen. https://doi.org/10.1037/xge0000433

Shmuel, A., Maier, A., 2015. Locally Measured Neuronal Correlates of Functional MRI Signals. In: Uludağ, K., Uğurbil, K., Berliner, L. (Eds.), fMRI: From Nuclear Spins to Brain Functions. Springer, New York, pp. 105-128

Simola, J., Le Fevre, K., Torniainen, J., Baccino, T., 2015. Affective processing in natural scene viewing: Valence and arousal interactions in eye-fixation-related potentials. Neuroimage 106, 21-33. https://doi.org/10.1016/j.neuroimage.2014.11.030

Smith, N.K., Cacioppo, J.T., Larsen, J.T., Chartrand, T.L., 2003. May I have your attention, please: Electrocortical responses to positive and negative stimuli. Neuropsychologia 41, 171-183

Soto, V., Tyson-Carr, J., Kokmotou, K., Roberts, H., Cook, S., Fallon, N., Giesbrecht, T., Stancak, A., 2018. Brain responses to emotional faces in natural settings: A wireless mobile EEG recording study. Frontiers in Psychology 9. https://doi.org/10.3389/fpsyg.2018.02003

Tavakoli, H.R., Atyabi, A., Rantanen, A., Laukka, S.J., Nefti-Meziani, S., Heikkila, J., 2015. Predicting the valence of a scene from observers' eye movements. PLoS One 10, e0138198. https://doi.org/10.1371/journal.pone.0138198

Telpaz, A., Webb, R., Levy, D.J., 2015. Using EEG to predict consumers' future choices. Journal of Marketing Research 52, 511-529. https://doi.org/10.1509/jmr.13.0564

Thickbroom, G.W., Mastaglia, F.L., 1986. Presaccadic spike potential. Relation to eye movement direction. Electroencephalography and Clinical Neurophysiology 64, 211-214

Tremblay, L., Schultz, W., 1999. Relative reward preference in primateorbitofrontal cortex. Nature 398, 704-708

Tyson-Carr, J., Kokmotou, K., Soto, V., Cook, S., Fallon, N., Giesbrecht, T., Stancak, A., 2018. Neural correlates of economic value and valuation context: an event-related potential study. J Neurophysiol 119, 1924-1933. https://doi.org/10.1152/jn.00524.2017

Tzovara, A., Chavarriaga, R., De Lucia, M., 2015. Quantifying the time for accurate EEG decoding of single value-based decisions. J Neurosci Methods 250, 114-125. https://doi.org/10.1016/j.jneumeth.2014.09.029

van der Laan, L.N., Hooge, I.T.C., de Ridder, D.T.D., Viergever, M.A., Smeets, P.A.M., 2015. Do you like what you see? The role of first fixation and total fixation duration in consumer choice. Food Quality and Preference 39, 46-55. https://doi.org/10.1016/j.foodqual.2014.06.015

Vecchiato, G., Cherubino, P., Maglione, A.G., Ezquierro, M.T.H., Marinozzi, F., Bini, F., Trettel, A., Babiloni, F., 2014. How to measure cerebral correlates of emotions in marketing relevant tasks. Cognitive Computation 6, 856-871. https://doi.org/10.1007/s12559-014-9304-x

Vecchiato, G., Toppi, J., Astolfi, L., De Vico Fallani, F., Cincotti, F., Mattia, D., Bez, F., Babiloni, F., 2011. Spectral EEG frontal asymmetries correlate with the experienced pleasantness of TV commercial advertisements. Med Biol Eng Comput 49, 579-583. https://doi.org/10.1007/s11517-011-0747-x

Wallis, J.D., Miller, E.K., 2003. Neuronal activity in primate dorsolateral and orbital prefrontal cortex during performance of a reward preference task. European Journal of Neuroscience 18, 2069-2081. https://doi.org/10.1046/j.1460-9568.2003.02922.x

Weber, B., Aholt, A., Neuhaus, C., Trautner, P., Elger, C.E., Teichert, T., 2007. Neural evidence for Reference-dependence in real-market-transactions. Neuroimage 35, 441-447. https://doi.org/10.1016/j.neuroimage.2006.11.034

Wilkinson, N., Klaes, M., 2012. An Introduction to Behavioral Economics. Palgrave Macmillan, Houndsmills, Basingstoke

Windmann, S., Kirsch, P., Mier, D., Stark, R., Walter, B., Gunturkun, O., Vaitl, D., 2006. On framing effects in decision making: Linking lateral versus medial orbitofrontal cortex activation to choice outcome processing. J Cogn Neurosci 18, 1198-1211. https://doi.org/10.1162/jocn.2006.18.7.1198

Yeung, N., Sanfey, A.G., 2004. Independent coding of reward magnitude and valence in the human brain. J Neurosci 24, 6258-6264. https://doi.org/10.1523/JNEUROSCI.4537-03.2004

Yu, R., Huang, Y., 2013. A nickel ain't worth a dime anymore: The illusion of money and the rapid encoding of its true value. PLoS One 8, e55025. https://doi.org/10.1371/journal.pone.0055025

Zald, D.H., McHugo, M., Ray, K.L., Glahn, D.C., Eickhoff, S.B., Laird, A.R., 2014. Meta-analytic connectivity modeling reveals differential functional connectivity of the medial and lateral orbitofrontal cortex. Cereb Cortex 24, 232-248. https://doi.org/10.1093/cercor/bhs308

Zhang, D., Luo, W., Luo, Y., 2013. Single-trial ERP analysis reveals facial expression category in a three-stage scheme. Brain Res 1512, 78-88. https://doi.org/10.1016/j.brainres.2013.03.044

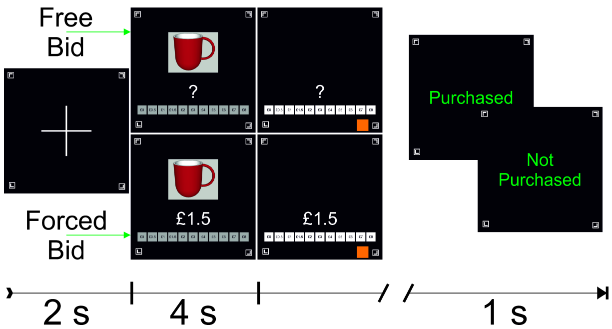
Free
Bid
?
?
Forced
Bid
£1.5
£1.5
Purchased
Not
Purchased
2 s
4 s
1 s

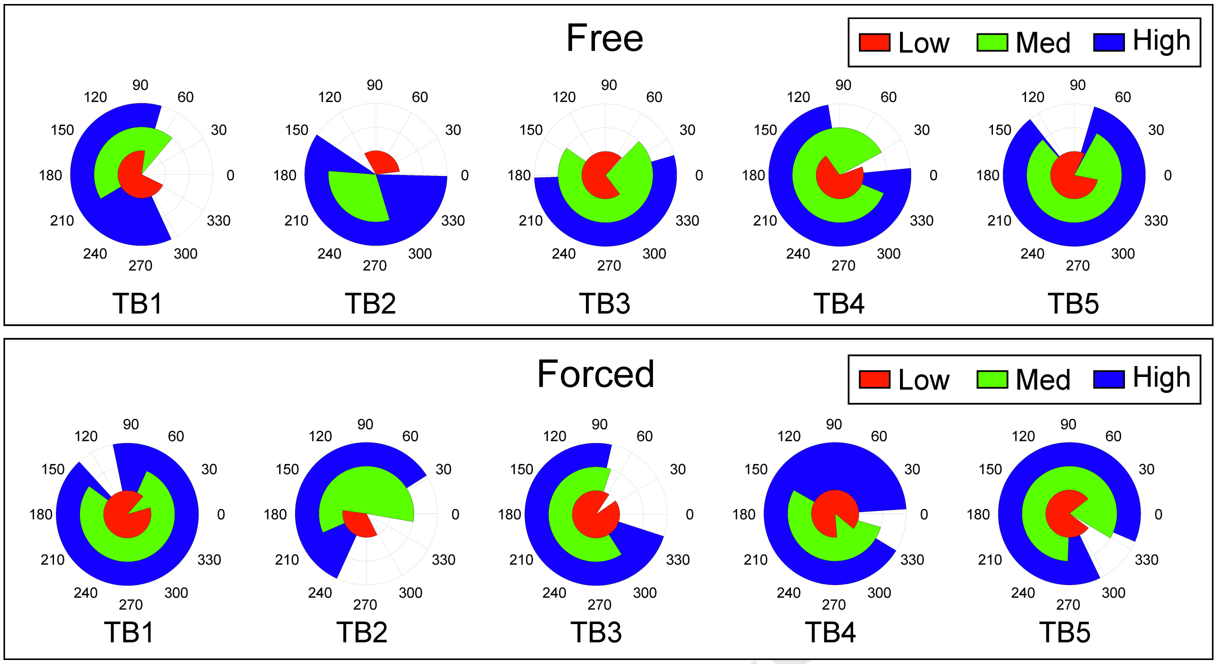
Free
Low
Med
High
90
60
30
0
330
300
270
240
210
180
150
120
TB1
TB2
TB3
TB4
TB5
Forced
Low
Med
High
TB1
TB2
TB3
TB4
TB5

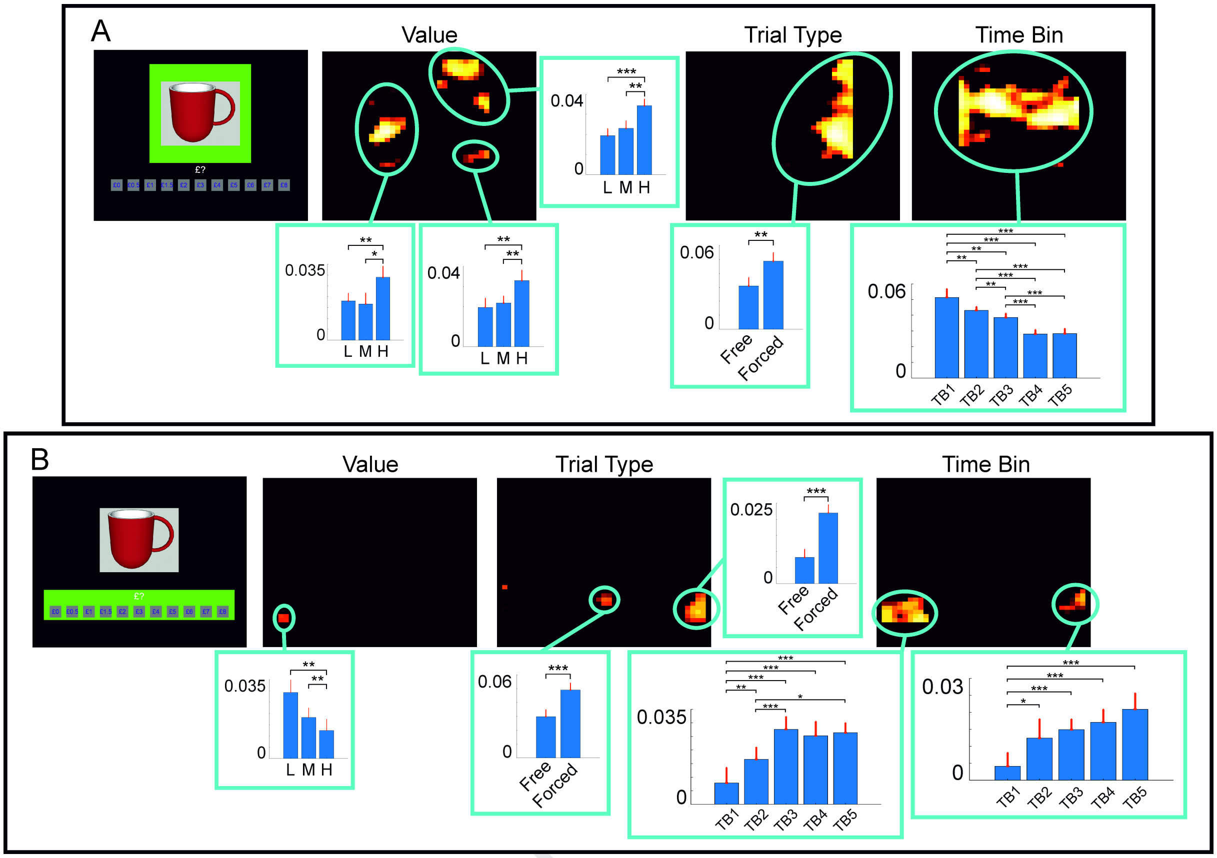

A
Value
0.04
0
L M H
Trial Type
Time Bin
0.035
0
L M H
0.04
0
L M H
0.06
0
Free
Forced
0.06
0
TB1
TB2
TB3
TB4
TB5
B
Value
Trial Type
0.025
0
Free
Forced
Time Bin
0.035
0
L M H
0.06
0
Free
Forced
0.035
0
TB1
TB2
TB3
TB4
TB5
0.03
0
TB1
TB2
TB3
TB4
TB5

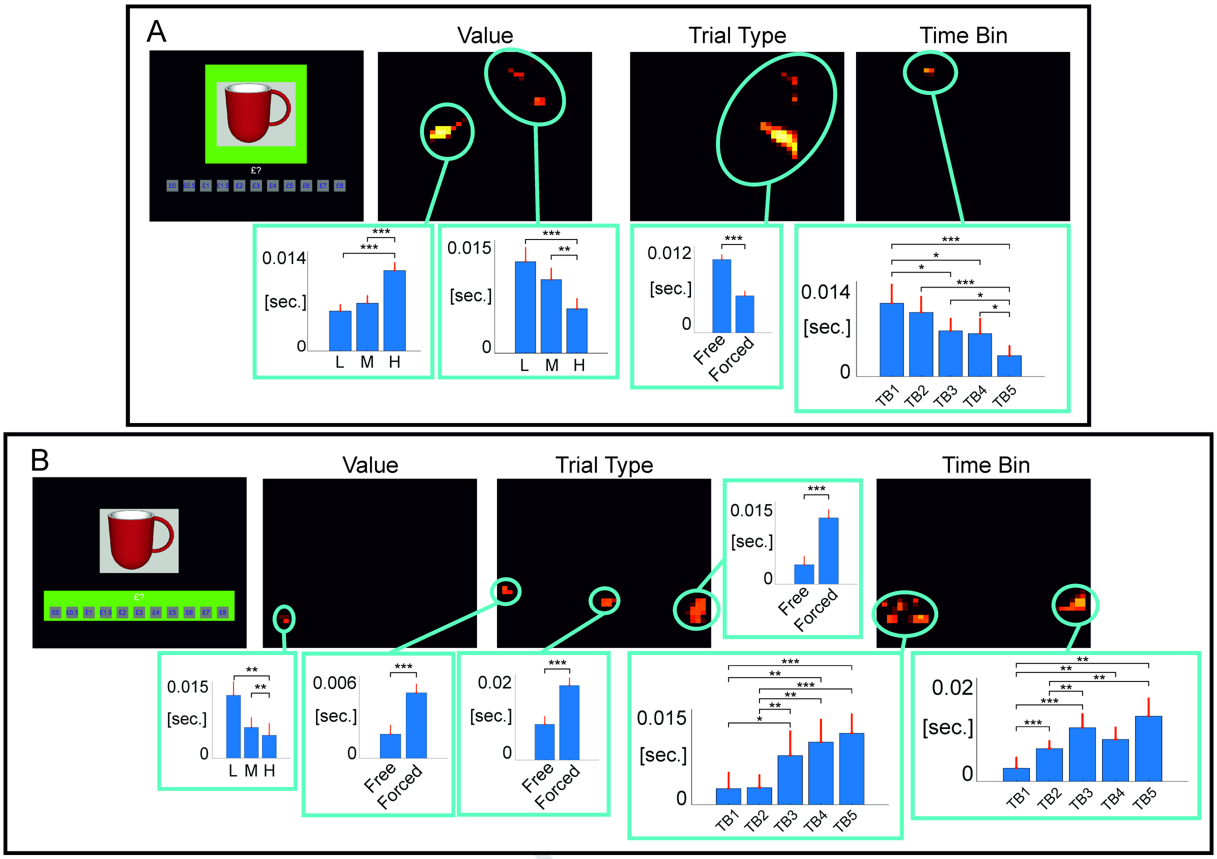

A
Value
Trial Type
Time Bin
0.014
[sec.]
0
L M H
0.015
[sec.]
0
L M H
0.012
[sec.]
0
Free
Forced
0.014
[sec.]
0
TB1 TB2 TB3 TB4 TB5
B
Value
Trial Type
Time Bin
0.015
[sec.]
0
Free
Forced
0.015
[sec.]
0
L M H
0.006
[sec.]
0
Free
Forced
0.02
[sec.]
0
Free
Forced
0.015
[sec.]
0
TB1 TB2 TB3 TB4 TB5
0.02
[sec.]
0
TB1 TB2 TB3 TB4 TB5

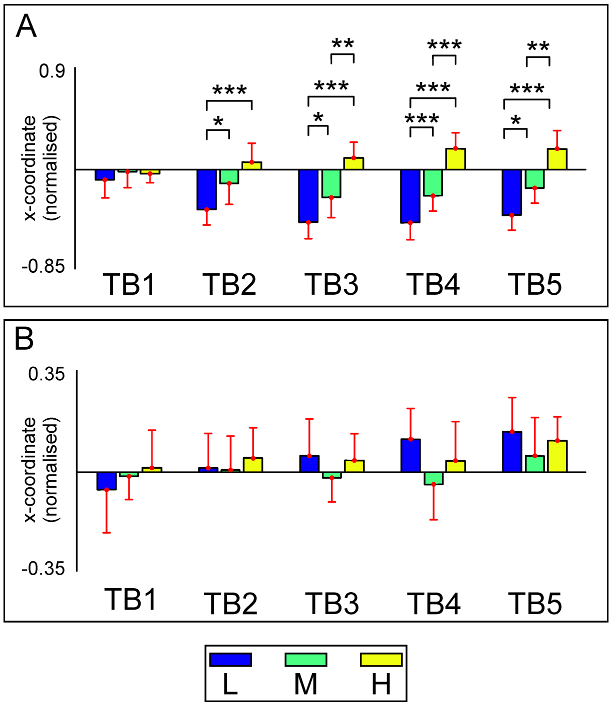
A
0.9
-0.85
x-coordinate (normalised)
*
***
**
***
TB1
TB2
TB3
TB4
TB5
B
0.35
-0.35
L
M
H

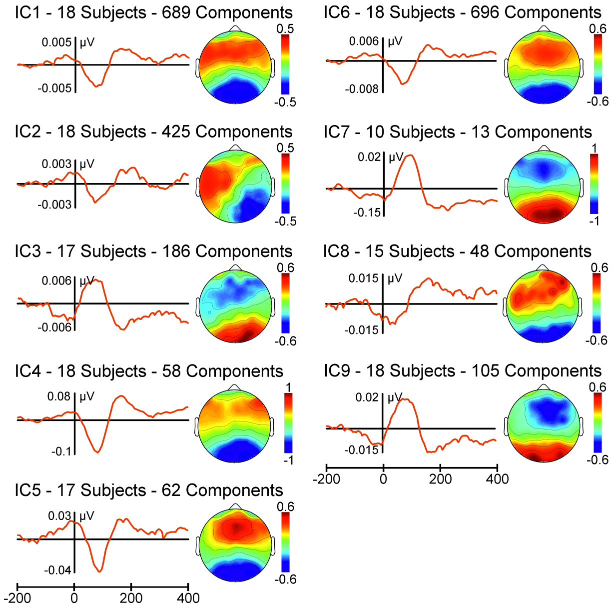

IC1 - 18 Subjects - 689 Components
IC2 - 18 Subjects - 425 Components
IC3 - 17 Subjects - 186 Components
IC4 - 18 Subjects - 58 Components
IC5 - 17 Subjects - 62 Components
IC6 - 18 Subjects - 696 Components
IC7 - 10 Subjects - 13 Components
IC8 - 15 Subjects - 48 Components
IC9 - 18 Subjects - 105 Components
μV
-200
0
200
400

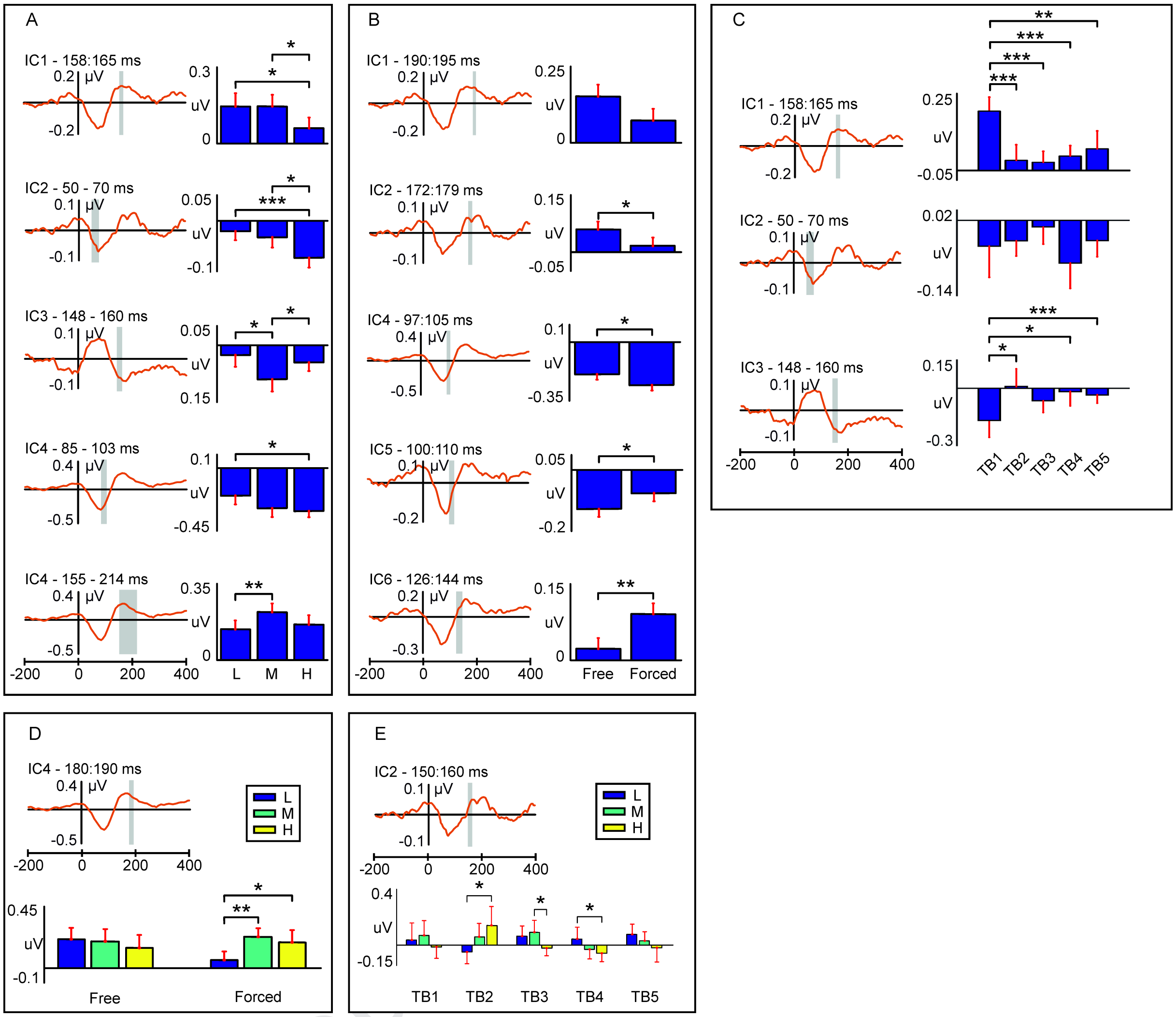

A
IC1 - 158:165 ms
IC2 - 50 - 70 ms
IC3 - 148 - 160 ms
IC4 - 85 - 103 ms
IC4 - 155 - 214 ms
L M H
B
IC1 - 190:195 ms
IC2 - 172:179 ms
IC4 - 97:105 ms
IC5 - 100:110 ms
IC6 - 126:144 ms
Free Forced
C
IC1 - 158:165 ms
IC2 - 50 - 70 ms
IC3 - 148 - 160 ms
TB1 TB2 TB3 TB4 TB5
D
IC4 - 180:190 ms
L
M
H
Free
Forced
E
IC2 - 150:160 ms
L
M
H
TB1 TB2 TB3 TB4 TB5